International Journal of Applied Mathematics and Computation
Vol. 4 No. 2 (December, 2018)

KALAHARI JOURNALS

Stagnation point flow of MHD micropolar fluid towards a vertical plate by surface heat flux

Animesh Adhikari(✉)[a]

[a]Department of Mathematics, Shyampur Siddheswari Mahavidyalaya, P.O.-Ajodhya, Howrah, West Bengal, 711312, India.

Received: 03rd August 2017 Revised: 14th April 2017 Accepted: 10th December 2017

ABSTRACT

A Magnetohydrodynamics (MHD) mixed convection stagnation point flow of an incompressible micropolar fluid towards a stretching vertical surface with prescribed surface heat flux is studied in this paper. The transformed differential equations are solved numerically by a finite-difference scheme, known as Keller-box method. Numerical results are obtained for the velocity, microrotation and temperature distribution for various parameters. Dual similarity solutions are found to exist for the opposing flow, while for the assisting flow, the solution is unique.

Keywords: micropolar fluid, stagnation point, similarity transformation, Keller box method.

1. Introduction

The theory of microrotation fluids, first studied by Eringen [1, 2], displays the effects of local rotary inertia and couple stresses, can explain the flow behavior due to the microscopic effects arising from the local structure and micromotions of the fluid elements in which the classical Newtonian fluids theory is inadequate. These fluids contain dilute suspensions of rigid micromolecules with individual motions which support stress and body moments and are influenced by spin-inertia. The theory of micropolar fluids and its extension to thermomicropolar fluids forms suitable non-Newtonian fluid models which can be used to analyze the behavior of exotic lubricants [3], polymeric fluids [4], liquid crystals [5], animal blood [6], colloidal suspensions, ferro-liquids etc. Kolpashchikov et al. [7] have derived a method to measure micropolar parameters experimentally. A thorough review of this subject and application of micropolar fluids mechanics has been provided by Ariman et al. [8]. Studies of the flow of heat convection in micropolar fluids have been focused on flat plate by Yucel [9], Jena and Mathur [10], Gorla [11], Hossain et al. [12] and Mori [13] etc. Several researchers have investigated the theory and its applications such as Lukaszewick [14], Eringen [15], Ishak et al. [16, 17] etc.

The study of MHD stagnation-point flow of an electrically conducting fluid is important in many practical applications such as cooling of nuclear reactors, cooling of electronic devices, extrusion of plastic sheets, paper production, glass blowing, metal spinning and drawing plastic films and many hydrodynamic processes. Laminar mixed convection in two-dimensional stagnation flows around heated surfaces in the case of arbitrary surface temperature and heat flux variations was examined by Ramachandran et al. [18]. They have established a reverse flow developed in the buoyancy opposing flow region and dual solutions are found to exist for a certain range of the buoyancy parameter. Devi et al. [19] extended this

✉ Corresponding author.
Email address: adhikarianimesh@gmail.com (Animesh Adhikari)

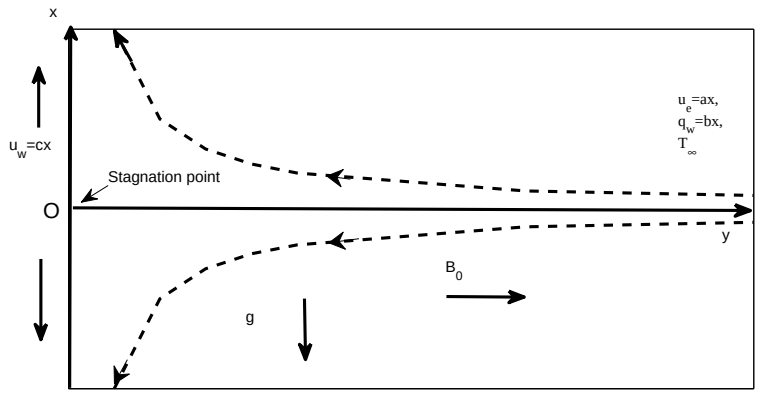

Figure 1: The sketch of the Problem

work for unsteady case. Lok et al. [20] studied the case for a vertical surface immersed in a micropolar fluid. Mahapatra and Gupta [21] studied the MHD stagnation point flow over a stretching surface. Chen [22] considered the combined effects of Joule heating and viscous dissipation on MHD flow past a permeable stretching surface with free convection and radiative heat transfer. Chin et al. [23], Ling et al. [24] and Ishak et al. [16, 17] reported the existence of dual solutions in the opposing flow case. Hydromagnetic thermal boundary layer flow of a perfectly conducting fluid was observed by Das [25]. Mukhopadhyay et al. [26] discussed Lie group analysis of MHD boundary layer slip flow past a heated stretching sheet in presence of heat source/sink. Shit and Halder [27] examined thermal radiation effects on MHD viscoelastic fluid flow over a stretching sheet with variable viscosity. Heat transfer effects on MHD viscous flow over a stretching sheet with prescribed surface heat flux was studied by Adhikari and Sanyal [28]. The study of boundary layer flows against a vertical surface problem were considered by Cramer [29], Cobble [30], Raptis et al. [31], Kumari et al. [32] and so many researchers.

2. Mathematical Formulation

Consider a steady, two-dimensional flow of an incompressible electrically conducting micropolar fluid toward a stagnation point past a vertical plate with prescribed surface heat flux. The frame of reference (x,y) is chosen such that the x-axis is along the direction of the surface and the y-axis is normal to the surface, as shown in Fig.1. It is assumed that the velocity of the flow external to the boundary layer $u_e(x)(= ax)$ and the surface heat flux $q_w(x)(= bx)$, temperature $T_w(x)$ of the plate are proportional to the distance x from the stagnation point, where a, b are constants. A uniform magnetic field of strength B_0 is assumed to be applied in the positive y-direction, normal to the vertical plate. The assisting flow situation occurs if the upper half of the flat surface is heated while the lower half of the flat surface is cooled. In this case the flow near the heated flat surface tends to move upward and the flow near the cooled flat surface tends to move downward. So this behaviour acts to assist the flow field. The opposing flow situation arises if the upper half of the flat surface is cooled while the lower half of the flat surface is heated.

The magnetic Reynolds number of the flow is taken to be small enough so that the induced magnetic field is negligible. Under the Boussinesq*'s* and the boundary layer approximations the governing

equations are given by

$$\frac{\partial u}{\partial x}+\frac{\partial v}{\partial y}=0, \tag{2.1}$$

$$u\frac{\partial u}{\partial x}+v\frac{\partial u}{\partial y}=u_e\frac{du_e}{dx}+\left(\frac{\mu+\kappa}{\rho}\right)\frac{\partial^2 u}{\partial y^2}+\frac{\kappa}{\rho}\frac{\partial N}{\partial y}+\frac{\sigma B_0^2}{\rho}(u_e-u)+g\beta(T-T_\infty), \tag{2.2}$$

$$\rho j\left(u\frac{\partial N}{\partial x}+v\frac{\partial N}{\partial y}\right)=\gamma\frac{\partial^2 N}{\partial y^2}-\kappa\left(2N+\frac{\partial u}{\partial y}\right), \tag{2.3}$$

$$u\frac{\partial T}{\partial x}+v\frac{\partial T}{\partial y}=\alpha\frac{\partial^2 T}{\partial y^2}. \tag{2.4}$$

Subject to the boundary conditions

$$at\ \ y=0: \quad u=u_w(x)=cx, \qquad v=v_w(x), \quad N=-n\frac{\partial u}{\partial y}, \qquad \frac{\partial T}{\partial y}=-\frac{q_w}{k}, \tag{2.5}$$

$$at \quad y\to\infty: \qquad u\to u_e(x)=ax, \qquad N\to 0, \qquad T\to T_\infty. \tag{2.6}$$

where u and v are the velocity components along the x and y-axis respectively, $u_w(x)$ the wall shrinking or stretching velocity ($c>0$ for stretching , $c<0$ for shrinking and $c=0$ for static wall), $v_w(x)$ the wall mass flux velocity, N is the microrotation or angular velocity whose direction of rotation is in the xy plane, μ is the dynamic viscosity, ρ is the density of the fluid, σ is the magnetic permeability, j is the micro-inertia per unit mass, i.e., micro-inertia density, γ is the spin gradient viscosity, κ is the vortex viscosity or micro-rotation viscosity, T is the fluid temperature in the boundary layer, T_∞ is the uniform ambient temperature, β is the thermal expansion coefficient, α is the thermal diffusivity, k is he thermal conductivity, q_w is the wall heat flux. Note that n is a constant such that $0\le n\le 1$. When $n=0$ then $N=0$ at the wall represents concentrated particle flows in which the microelements close to the wall surface are unable to rotate. This case is also known as the strong concentration of microelements. When $n=1/2$, we have the vanishing of anti-symmetric part of the stress tensor and denotes weak concentration of microelements, the case $n=1$ is used for the modeling of turbulent boundary layer flows. We shall consider here both cases of $n=0$ and $n=1/2$. Assume $\gamma=\left(\mu+\frac{\kappa}{2}\right)j=\mu\left(1+\frac{K}{2}\right)j, \quad where\ K=\frac{\kappa}{\mu}$ is the micropolar or material parameter. This assumption is invoked to allow the field of equations that predicts the correct behavior in the limiting case when the microstructure effects become negligible and the total spin N reduces to the angular velocity [9, 33].
Introduce a Stream function Ψ as follows

$$u=\frac{\partial\Psi}{\partial y}, \quad v=-\frac{\partial\Psi}{\partial x}, \tag{2.7}$$

The momentum, angular momentum and energy equations can be transformed into the corresponding ordinary differential equations by the following transformation:

$$\eta=\sqrt{\frac{a}{\nu}}\,y, f(\eta)=\frac{\Psi}{x\sqrt{a\nu}}, p(\eta)=\frac{N}{ax\sqrt{\frac{a}{\nu}}}, \quad \theta(\eta)=\frac{k(T-T_\infty)}{q_w}\sqrt{\frac{a}{\nu}}, \tag{2.8}$$

where η the independent dimensionless similarity variable. Thus u and v are given by $u = axf'(\eta)$, $v = -\sqrt{a\nu}\ f(\eta)$. Substituting variables (2.8) into equations (2.2) to (2.4), we get the following ordinary differential equations:

$$(1+K)\,f'''+ff''+1-f'^2+Kp+M\,(1-f')+\lambda\theta=0, \tag{2.9}$$

$$\left(1+\frac{K}{2}\right)p''+fp'-pf'-K\,(2p+f'')=0, \tag{2.10}$$

$$\frac{1}{P_r}\theta''+f\theta'-\theta f'=0, \tag{2.11}$$

subject to the boundary conditions (2.5) & (2.6) which become

$$f(0)=s,\quad f'(0)=e,\quad p(0)=-nf''(0),\quad \theta'(0)=-1, \tag{2.12}$$

$$f'(\eta)\to 1,\quad p(\eta)\to 0,\qquad \theta(\eta)\to 0\quad as\quad \eta\to\infty. \tag{2.13}$$

Here $f'(\eta)$, $p(\eta)\,and\,\theta(\eta)$ stand for (dimensionless) the velocity, the angular velocity and temperature respectively. In the above equations, primes denote differentiation with respect to η; $j=\frac{\nu}{a}$ thecharacteristic length [34], P_r=$\frac{\nu}{\alpha}$ the Prandtl number, $M=\frac{\sigma B_0^2}{\rho a}$ the magnetic parameter, e=c/a the velocity ratio parameter, $s=-\frac{v_w(x)}{\sqrt{a\nu}}$ the constant mass flux with s>0 for suction and s<0 for injection, $\lambda=\frac{Gr_x}{Re_x^{5/2}}$ the buoyancy or mixed convection parameter, $Gr_x=\frac{g\beta(T_w-T_\infty)x^3}{\nu^2}$ the local Grashof number and $Re_x=\frac{Ux}{\nu}$ is the local Reynolds number. Here λ is a constant and the negative and positive values of λ correspond to the opposing and assisting flows respectively. When λ=0, i.e., when T_w=T_∞ we get the pure forced convection flow. Ramchandran et al. [18] considered the present problem with $M=0$ and $K=0$.

The skin friction coefficient C_f and the local Nusselt number Nu_x are defined as

$$C_f=\frac{\tau_w}{\rho U^2/2}, Nu_x=\frac{xq_w}{k(T_w-T_\infty)}, \tag{2.14}$$

where the wall shear stress τ_w and the heat flux q_w are given by

$$\tau_w=\left[(\mu+\kappa)\frac{\partial u}{\partial y}+\kappa N\right]_{y=0}, q_w=-k\left[\frac{\partial T}{\partial y}\right]_{y=0}, \tag{2.15}$$

with k being the thermal conductivity. Using the similarity variables (2.8), we get

$$\frac{1}{2}C_fRe_x^{1/2}=\left[1+(1-n)\frac{K}{2}\right]f''(0), \frac{Nu_x}{Re_x^{1/2}}=\frac{1}{\theta(0)}. \tag{2.16}$$

3. Numerical Solutions

The equations (2.9), (2.10) and (2.11) subject to the boundary conditions (2.12) and (2.13) are solved numerically using an implicit finite-difference scheme known as the Keller-box method [35]. The method has following four basic steps:

1. Reduce Equations (2.9), (2.10) and (2.11) to first order equations;
2. Write the difference equations using central differences;
3. Linearise the resulting algebraic equations by Newton's method and write them in Matrix-vector form;
4. Use the Block-tridiagonal elimination technique to solve the linear system.

3.1 *The Finite-Difference Scheme*

In this section, steps (i) and (ii) are combined. First we introduce new dependent variables u(x,η), v(x,η), g(x,η) and q(x,η) such that

$$f' = u, \quad u' = v, \quad p' = g, \quad \theta' = q, \tag{3.1}$$

so that equations (2.9), (2.10) and (2.11) reduce to

$$(1+K)\,v' + fv + 1 - u^2 + Kg + M\,(1-u) + \lambda\theta = 0, \tag{3.2}$$

$$\left(1+\frac{K}{2}\right) g' + fg - up - K\,(2p+v) = 0, \tag{3.3}$$

$$\frac{1}{P_r} q' + fq - u\theta = 0. \tag{3.4}$$

We now consider the net rectangle in the x-η plane as shown in fig.2 and the net points defined as follows:

$$x^0 = 0, \quad x^n = x^{n-1} + k_n, \quad n = 1, 2, \ldots N; \tag{3.5}$$

$$\eta_0 = 0, \quad \eta_j = \eta_{j-1} + h_j, \quad j = 1, 2, \ldots J; \quad \eta_j = \eta_\infty, \tag{3.6}$$

where k_n is the Δx-spacing and h_j is the $\Delta\eta$-spacing. Here n and j are just the sequence of numbers that indicate the coordinate location, not tensor indices or exponents.
Here we use the following finite-differences:

$$()^n_{j-1/2} = \frac{1}{2}\left[()^n_j + ()^n_{j-1}\right], \tag{3.7}$$

$$()^{n-1/2}_j = \frac{1}{2}\left[()^n_j + ()^{n-1}_j\right]. \tag{3.8}$$

$$\left(\frac{\partial u}{\partial x}\right)^{n-1/2}_{j-1/2} = \frac{1}{k_n}\left[(u)^n_{j-1/2} - (u)^{n-1}_{j-1/2}\right], \tag{3.9}$$

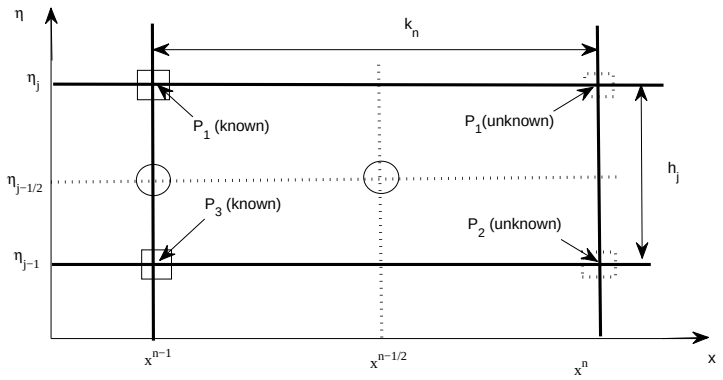

Figure 2: Net Rectangle difference

$$\left(\frac{\partial u}{\partial \eta}\right)_{j-1/2}^{n-1/2} = \frac{1}{h_j}\left[(u)_j^{n-1/2} - (u)_{j-1}^{n-1/2}\right]. \tag{3.10}$$

Now we write the finite-difference for the midpoint $\left(x^n,\, \eta_{j-1/2}\right)$ of the segment P_1P_2 using (3.7)-(3.10). This process is called "centering about$\left(x^n,\, \eta_{j-1/2}\right)$". We get by omitting upper indices n:

$$f_j - f_{j-1} - \frac{h_j}{2}\left(u_j + u_{j-1}\right) = 0, \tag{3.11}$$

$$u_j - u_{j-1} - \frac{h_j}{2}\left(v_j + v_{j-1}\right) = 0, \tag{3.12}$$

$$p_j - p_{j-1} - \frac{h_j}{2}\left(g_j + g_{j-1}\right) = 0, \tag{3.13}$$

$$\theta_j - \theta_{j-1} - \frac{h_j}{2}\left(q_j + q_{j-1}\right) = 0, \tag{3.14}$$

$$(1+K)\frac{(v_j - v_{j-1})}{h_j} + \frac{(f_j + f_{j-1})}{2}.\frac{(v_j + v_{j-1})}{2} + 1 - \frac{(u_j + u_{j-1})^2}{4} + K\frac{(g_j + g_{j-1})}{2}$$

$$+M\left(1 - \frac{(u_j + u_{j-1})}{2}\right) + \lambda\frac{(\theta_j + \theta_{j-1})}{2} = 0, \tag{3.15}$$

$$\left(1 + \frac{K}{2}\right)\frac{(g_j - g_{j-1})}{h_j} + \frac{(g_j + g_{j-1})}{2}\frac{(f_j + f_{j-1})}{2} - \frac{(u_j + u_{j-1})}{2}\frac{(p_j + p_{j-1})}{2}$$

$$-K\left[2\frac{(p_j+p_{j-1})}{2}+\frac{(v_j+v_{j-1})}{2}\right]=0, \tag{3.16}$$

$$\frac{1}{P_r}\frac{(q_j-q_{j-1})}{h_j}+\frac{(f_j+f_{j-1})}{2}\frac{(q_j+q_{j-1})}{2}-\frac{(u_j+u_{j-1})}{2}\frac{(\theta_j+\theta_{j-1})}{2}=0. \tag{3.17}$$

The boundary conditions at x=x^n are

$$f_0^n=0,\ \ u_0^n=0,\ \ p_0^n=-nv_0^n,\ \ q_0^n=-1,\ u_J^n=1,\ \ p_J^n=0,\ \ \theta_J^n=0\ . \tag{3.18}$$

3.2 *Newton's method for linearisation*

To linearise the nonlinear system (3.11)-(3.17), we introduce the following i-th iterate at x=x^n:

$$f_j^{(i+1)}=f_j^{(i)}+\delta f_j^{(i)},\quad u_j^{(i+1)}=u_j^{(i)}+\delta u_j^{(i)},$$
$$v_j^{(i+1)}=v_j^{(i)}+\delta v_j^{(i)},\ p_j^{(i+1)}=p_j^{(i)}+\delta p_j^{(i)},$$
$$g_j^{(i+1)}=g_j^{(i)}+\delta g_j^{(i)},\ \theta_j^{(i+1)}=\theta_j^{(i)}+\delta\theta_j^{(i)},$$

$$q_j^{(i+1)}=q_j^{(i)}+\delta q_j^{(i)}. \tag{3.19}$$

Substituting these in (3.11)-(3.17), then drop the quadratic and higher-order terms in $\delta f_j^{(i)}$, $\delta u_j^{(i)}$, $\delta v_j^{(i)}$, $\delta p_j^{(i)}$, $\delta g_j^{(i)}$, $\delta\theta_j^{(i)}$ *and* $\delta q_j^{(i)}$, we get the following linear tridiagonal system:

$$\delta f_j-\delta f_{j-1}-\frac{1}{2}h_j\,(\delta u_j+\delta u_{j-1})=(r_1)_j, \tag{3.20}$$

$$\delta u_j-\delta u_{j-1}-\frac{1}{2}h_j\,(\delta v_j+\delta v_{j-1})=(r_2)_j, \tag{3.21}$$

$$\delta p_j-\ \delta p_{j-1}-\frac{1}{2}h_j\,(\delta g_j+\delta g_{j-1})=(r_3)_j, \tag{3.22}$$

$$\delta\theta_j-\delta\theta_{j-1}-\frac{1}{2}h_j\,(\delta q_j+\delta q_{j-1})=(r_4)_j, \tag{3.23}$$

$$(a_1)_j\delta f_j+(a_2)_j\delta f_{j-1}+(a_3)_j\delta u_j+(a_4)_j\delta u_{j-1}+(a_5)_j\delta v_j+(a_6)_j\delta v_{j-1}+(a_7)_j\delta g_j +(a_8)_j\delta g_{j-1}+(a_9)_j\delta\theta_j+(a_{10})_j\delta\theta_{j-1}=(r_5)_j, \tag{3.24}$$

$$(b_1)_j\delta f_j+(b_2)_j\delta f_{j-1}+(b_3)_j\delta u_j+(b_4)_j\delta u_{j-1}+(b_5)_j\delta v_j+(b_6)_j\delta v_{j-1}+(b_7)_j\delta p_j +(b_8)_j\delta p_{j-1}+(b_9)_j\delta g_j+(b_{10})_j\delta g_{j-1}=(r_6)_j, \tag{3.25}$$

$$(c_1)_j\delta f_j+(c_2)_j\delta f_{j-1}+(c_3)_j\delta u_j+(c_4)_j\delta u_{j-1}+(c_5)_j\delta\theta_j+(c_6)_j\delta\theta_{j-1}+(c_7)_j\delta q_j \\ +(c_8)_j\delta q_{j-1}=(r_7)_j, \tag{3.26}$$

where

$$(a_1)_j=\frac{1}{2}v_{j-1/2}=(a_2)_j, \qquad (a_3)_j=-\left(u_{j-1/2}+\frac{M}{2}\right)=(a_4)_j\ ,$$

$$(a_5)_j=\frac{1+K}{h_j}+\frac{1}{2}f_{j-1/2}, \quad (a_6)_j=-\frac{(1+K)}{h_j}+\frac{1}{2}f_{j-1/2}\ ,\ (a_7)_j=\frac{K}{2}=(a_8)_j$$

$$(a_9)_j=\frac{\lambda}{2}=(a_{10})_j\ ,(b_1)_j=\frac{1}{2}g_{j-1/2}=(b_2)_j\ ,\ (b_3)_j=-\frac{1}{2}p_{j-1/2}=(b_4)_j,$$

$$(b_5)_j=-\frac{K}{2}=(b_6)_j, \quad (b_7)_j=-\left(\frac{u_{j-1/2}}{2}+K\right)=(b_8)_j\ ,\ (b_9)_j=\frac{1}{h_j}\left(1+\frac{K}{2}\right)+\frac{1}{2}f_{j-1/2}$$

$$(b_{10})_j=-\frac{1}{h_j}\left(1+\frac{K}{2}\right)+\frac{1}{2}f_{j-1/2}\ ,(c_1)_j=\frac{1}{2}q_{j-1/2}=(c_2)_j\ ,\ (c_3)_j=-\frac{1}{2}\theta_{j-1/2}=(c_4)_j\ ,$$

$$(c_5)_j=-\frac{1}{2}u_{j-1/2}=(c_6)_j\ ,\ (c_7)_j=\frac{1}{P_rh_j}+\frac{1}{2}f_{j-1/2},(c_8)_j=-\frac{1}{P_rh_j}+\frac{1}{2}f_{j-1/2},$$

$$(r_1)_j=f_{j-1}-f_j+h_ju_{j-1/2}, \quad (r_2)_j=u_{j-1}-u_j+h_jv_{j-1/2},$$

$$(r_3)_j=p_{j-1}-p_j+h_jg_{j-1/2}, \quad (r_4)_j=\theta_{j-1}-\theta_j+h_jq_{j-1/2},$$

$$(r_5)_j=-\frac{1}{h_j}(1+K)(v_j-v_{j-1})-f_{j-\frac{1}{2}}v_{j-\frac{1}{2}}-(1+M)+\left(u_{j-\frac{1}{2}}\right)^2-Kg_{j-\frac{1}{2}}+Mu_{j-\frac{1}{2}}-\lambda\theta_{j-\frac{1}{2}},$$

$$(r_6)_j=-\frac{1}{h_j}\left(1+\frac{K}{2}\right)(g_j-g_{j-1})-g_{j-1/2}f_{j-1/2}+u_{j-1/2}p_{j-\frac{1}{2}}+2Kp_{j-1/2}+Kv_{j-1/2}\ ,$$

$$(r_7)_j=-\frac{1}{P_rh_j}(q_j-q_{j-1})-f_{j-1/2}q_{j-1/2}+u_{j-1/2}\theta_{j-1/2}. \tag{3.27}$$

For all iterates, we take

$$\delta f_0=0,\ \delta u_0=0,\ \ \delta p_0=0,\ \delta q_0=0,\ \delta u_J=0,\ \ \delta p_J=0,\ \ \delta\theta_J=0, \tag{3.28}$$

3.3 *The block tridiagonal matrix*

The linearised difference system (3.20)-(3.26) has a block tridiagonal structure as follows:

$$\begin{bmatrix} [A_1] & [C_1] & \cdots & & & \\ [B_2] & [A_2] & [C_2] & \cdots & & \\ \cdot & \cdots & \cdots & \cdot & \cdot & \\ \cdot & \cdot & \cdots & \cdot & \cdot & \\ \cdot & \cdot & \cdot & [B_{J-1}] & [A_{J-1}] & [C_{J-1}] \\ \cdot & \cdots & \cdot & \cdots & [B_J] & [A_J] \end{bmatrix} \begin{bmatrix} [\delta_1] \\ [\delta_2] \\ \cdot \\ \cdot \\ [\delta_{J-1}] \\ [\delta_J] \end{bmatrix} = \begin{bmatrix} [r_1] \\ [r_2] \\ \cdot \\ \cdot \\ [r_{J-1}] \\ [r_J] \end{bmatrix}$$

that is:

$$\mathbf{A}\delta=\mathbf{r} \tag{3.29}$$

where

$$[A_1] = \begin{bmatrix} 0 & 0 & 0 & 1 & 0 & 0 & 0 \\ d & 0 & 0 & 0 & d & 0 & 0 \\ 0 & d & 0 & 0 & 0 & d & 0 \\ 0 & 0 & -1 & 0 & 0 & 0 & d \\ (a_6)_j & (a_8)_j & (a_{10})_j & (a_1)_j & (a_5)_j & (a_7)_j & 0 \\ (b_6)_j & (b_{10})_j & 0 & (b_1)_j & (b_5)_j & (b_9)_j & 0 \\ 0 & 0 & (c_6)_j & (c_1)_j & 0 & 0 & (c_7)_j \end{bmatrix},$$

$$[A_j] = \begin{bmatrix} d & 0 & 0 & 1 & 0 & 0 & 0 \\ -1 & 0 & 0 & 0 & d & 0 & 0 \\ 0 & -1 & 0 & 0 & 0 & d & 0 \\ 0 & 0 & -1 & 0 & 0 & 0 & d \\ (a_4)_j & 0 & (a_{10})_j & (a_1)_j & (a_5)_j & (a_7)_j & 0 \\ (b_4)_j & (b_8)_j & 0 & (b_1)_j & (b_5)_j & (b_9)_j & 0 \\ (c_4)_j & 0 & (c_6)_j & (c_1)_j & 0 & 0 & (c_7)_j \end{bmatrix}; \quad 2 \le j \le J$$

$$[B_j] = \begin{bmatrix} 0 & 0 & 0 & -1 & 0 & 0 & 0 \\ 0 & 0 & 0 & 0 & d & 0 & 0 \\ 0 & 0 & 0 & 0 & 0 & d & 0 \\ 0 & 0 & 0 & 0 & 0 & 0 & d \\ 0 & 0 & 0 & (a_2)_j & (a_6)_j & (a_8)_j & 0 \\ 0 & 0 & 0 & (b_2)_j & (b_6)_j & (b_{10})_j & 0 \\ 0 & 0 & 0 & (c_2)_j & 0 & 0 & (c_8)_j \end{bmatrix}; \quad 2 \le j \le J$$

$$[C_j] = \begin{bmatrix} d & 0 & 0 & 0 & 0 & 0 & 0 \\ 1 & 0 & 0 & 0 & 0 & 0 & 0 \\ 0 & 1 & 0 & 0 & 0 & 0 & 0 \\ 0 & 0 & 1 & 0 & 0 & 0 & 0 \\ (a_3)_j & 0 & (a_9)_j & 0 & 0 & 0 & 0 \\ (b_3)_j & (b_7)_j & 0 & 0 & 0 & 0 & 0 \\ (c_3)_j & 0 & (c_5)_j & 0 & 0 & 0 & 0 \end{bmatrix}, 1 \le j \le J-1$$

where $d = -\frac{h_j}{2}$, $[\delta_1] = \begin{bmatrix} \delta v_0 \\ \delta g_0 \\ \delta \theta_0 \\ \delta f_1 \\ \delta v_1 \\ \delta g_1 \\ \delta q_1 \end{bmatrix}$, $[\delta_j] = \begin{bmatrix} \delta u_{j-1} \\ \delta p_{j-1} \\ \delta \theta_{j-1} \\ \delta f_j \\ \delta v_j \\ \delta g_j \\ \delta q_j \end{bmatrix}$, $2 \le j \le J$; $[r_j] = \begin{bmatrix} (r_1)_j \\ (r_2)_j \\ (r_3)_j \\ (r_4)_j \\ (r_5)_j \\ (r_6)_j \\ (r_7)_j \end{bmatrix}$, $1 \le j \le J$.

Forward sweep: To solve Equation (3.29), assume the matrix **A** is nonsingular and it can be factored into

$$A = LU, \tag{3.30}$$

where

$$L=\begin{bmatrix} [\alpha_1] & 0 & \ldots..\ 0\ 0 \\ [B_2] & [\alpha_2] & \ldots\ldots\ 0\ 0 \\ \ldots. & \ldots. & \ldots..\ \ldots\ \ldots. \\ 0 & 0 & \ldots\ [\alpha_{J-1}]\ 0 \\ 0 & 0 & \ldots\ [B_J]\ [\alpha_J] \end{bmatrix}, U=\begin{bmatrix} [I] & [\Gamma_1] & \ldots..\ & 0 & 0 \\ 0 & [I] & [\Gamma_2]\ldots.\ 0 & & 0 \\ \ldots. & \ldots. & \ldots..\ \ldots\ \ldots. & & \\ 0 & 0 & \ldots & [I] & [\Gamma_{J-1}] \\ 0 & 0 & \ldots & 0 & [I] \end{bmatrix}$$

[I] is the identity matrix of order 7, and $[\alpha_j]$, $[\Gamma_j]$are 7x7 matrices whose elements are determined by the following equations:

$$[\alpha_1]=[A_1],$$
$$[A_1]\,[\Gamma_1]=[C_1],$$
$$[\alpha_j]=[A_j]-[B_j]\,[\Gamma_{j-1}], \quad j=2,3,\ldots.J$$
$$[\alpha_j]\,[\Gamma_j]=[C_j], \quad j=2,3,\ldots\ldots J-1$$

Backward Sweep: Equation (3.30) can now be substituted in (3.29) and we get

$$\mathbf{LU}\delta=\mathbf{r}, \tag{3.31}$$

Let

$$\mathbf{U}\delta=\mathbf{w}, \tag{3.32}$$

Then Eq. (3.31) becomes

$$\mathbf{Lw}=\mathbf{r}, \tag{3.33}$$

where

$$\mathbf{w}=\begin{bmatrix} [w_1] \\ [w_2] \\ \ldots. \\ [w_{J-1}] \\ [w_J] \end{bmatrix},$$

And the $[w_j]$ are 7x1 column matrices. The elements $\mathbf{w}$ can be solved from the equation (3.33) by

$$[\alpha_1]\,[w_1]=[r_1], \tag{3.34}$$

$$[\alpha_j]\,[w_j]=[r_j]-[B_j]\,[w_{j-1}], \quad 2\le j\le J \tag{3.35}$$

By these $[w_j]$, from the Eq.(3.32) we get $[\delta_j]$:

$$[\delta_J]=[w_J], \tag{3.36}$$

$$[\delta_j]=[w_j]-[\Gamma_j]\,[\delta_{j+1}] \ , \qquad 1\le j\le J-1 \tag{3.37}$$

These iterations will be stopped when

$$\left|\delta v_0^{(i)}\right|<\epsilon, \tag{3.38}$$

where ε is the desired level of accuracy.

Table 1: Values of $f''(0)$ and $1/\theta(0)$ for different values of Pr (when λ=1, K=0, n=0.5, M=0, e=0, s=0, ? η=0.02)

Pr	Bachok & Ishak(2009)		Present result	
	$f''(0)$	$1/\theta(0)$	$f''(0)$	$1/\theta(0)$
0.7	1.8339	0.7776	1.8339	0.7776
1.0	1.7338	0.8781	1.7339	0.8781
7.0	1.4037	1.6913	1.4037	1.6916
10.0	1.3711	1.9067	1.3711	1.9072

Table 2: Critical values of λ (i.e., λ_c)

	s		M		K	
	0	1	0	0.5	0	1
λ_c	-2.7	-8.07	-4.01	-4.68	-4.13	-5.16

4. Results and Discussion

The step size $\Delta\eta$ of η and the edge of the boundary layer η_∞ had to be adjusted for different values of parameters to maintain accuracy within the interval $0 \leq \eta \leq \eta_\infty$, where η_8 is the non-dimensionalised boundary layer thickness, we run the programme in MATLAB upto the desired level of accuracy. The validity of the numerical results has been compared with the results of Bachok and Ishak [36] and they are found to be in a very good agreement, as presented in Table 1.

The variation of skin friction coefficient $f''(0)$ and the local Nusselt number $1/\theta(0)$ with λ for different values of the suction parameter s, the magnetic parameter M and the material parameter K are given by figures 3 to 8 respectively. The dual solutions were obtained by setting two different values of η_∞, which produce two different velocity and temperature profiles both satisfy the boundary conditions. It is seen that for the opposing flow (λ<0) dual solutions are found to exist for the values of s, M and K considered. For a particular value of s, M and K the solution is present up to a critical value of λ, say λ_c, outside which the boundary layer separates from the surface and the solution based upon the boundary-layer approximations are not feasible. It is clear from the figures 3 to 8 that larger values of s, M and K enhance the range of λ for which the solution exists. In this study the critical values of λ (λ_c) are given by the Table 2.

Hence the boundary-layer separation is delayed with increase of s, M and K. So suction and Magnetic field holdup the boundary layer separation respectively compared to the no-suction (s=0) and non-magnetic field (M=0) cases. Similarly micropolar fluids ($K \neq 0$) delay the boundary-layer separation as compared to the classical Newtonian fluids (K=0). Figures 3, 5 and 7 respectively depict that the value of $|f''(0)|$decreases as s, M and K increase, thus suction, magnetic field and micropolar fluids show drag reduction compared to the no-suction, non-magnetic field and classical Newtonian fluids respectively.

Figures 9-11 display the dual solutions for the opposing flow for different values of s, where the first solutions are stable with the most physically relevance while the second solutions are not. The region of reversed flow exists for the case of the second solutions from figure 9 and this would unacceptable as possible asymptotic solutions to which a fully forward flow developing near the stagnation point could grow.

The velocity, angular velocity and temperature profiles for both assisting (λ=1) and opposing flow (λ=-1) are given in the figures 12 to 14 for different values of the suction parameter s respectively. Here Pr=0.7, M=0.5, K=0.5, n=0.5, e=0.5. Figure 12 depicts that the velocity profiles decrease for the assisting flow but the profile increase for the opposing flow with the increase of s. For the assisting flow angular velocity profiles increase near boundary but after a certain point the profiles decrease with

the increasing of s and for the opposing flow the profiles increase with s (fig.13). Temperature profiles decrease with the increase of s for the both flows. When injection occurs (s=-1) temperature profile for the assisting flow is lower compared to the opposing flow but when suction occurs (s=1) temperature profiles are same for the both flows (fig. 14).

The effects of the material parameter K on the velocity, angular velocity and temperature profiles are respectively shown by the figures 15 to 17. Figure 15 describes that the velocity profiles decrease with the increase of K for the both flows. Angular velocity profiles decrease with the increasing of K and for the Newtonian fluid (K=0) the profiles are same for the both flows (fig.16). When K=1 angular velocity profile for the assisting flow is higher than the opposing flow but the reverse result occurs when K=-0.9. Temperature profiles decrease with the increase of K for the assisting flows (fig.17).

Figures 18 and 19 respectively display the effects of the magnetic parameter M on the velocity and angular velocity profiles. The figures respectively describe that the velocity and angular velocity profiles increase with the increase of M for the both flows.

The effects of the Prandtl number Pr on the velocity, angular velocity and temperature profiles are respectively shown by the figures 20 to 22. Figure 20 depicts that the velocity profiles decrease for the assisting flow but the profile increase for the opposing flow with the increase of Pr. For the assisting flow angular velocity profiles increase near boundary but after a certain point the profiles decrease with the increasing of Pr but the reverse results hold for the opposing flow. When Pr=10 the velocity and angular velocity profiles are same for the both flows (fig.21). Temperature profiles decrease with the increase of Pr for the both flows. When Pr=0.1 temperature profile for the assisting flow is lower compared to the opposing flow but when Pr=0.7 or 1, temperature profiles are same for the both flows (fig. 22).

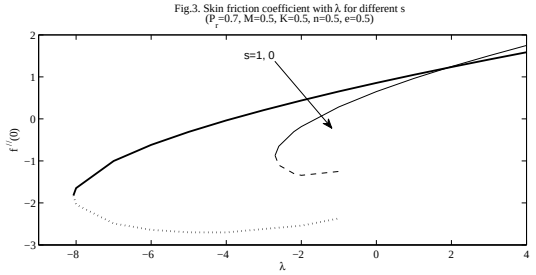

Figure 3

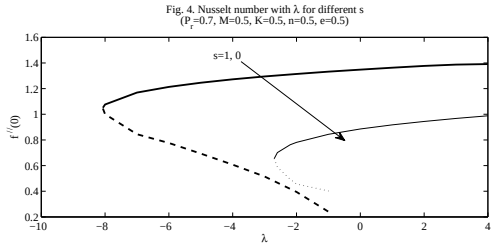

Figure 4

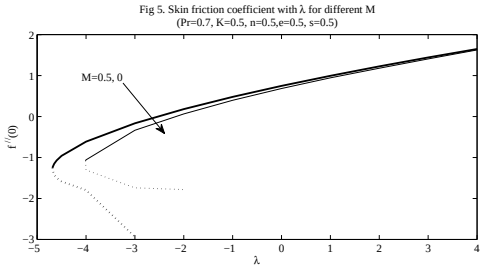

Figure 5

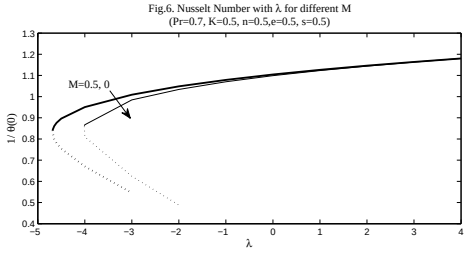

Figure 6

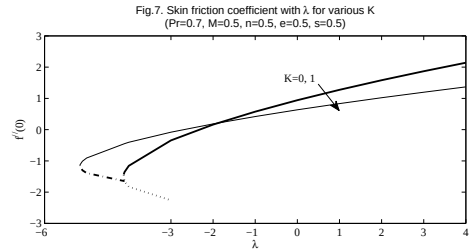

Figure 7

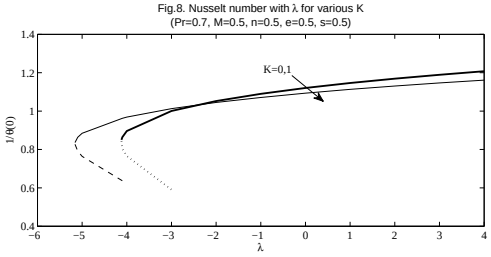

Figure 8

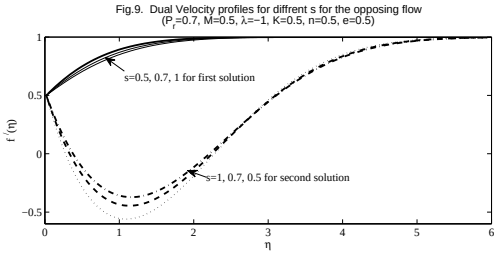

Figure 9

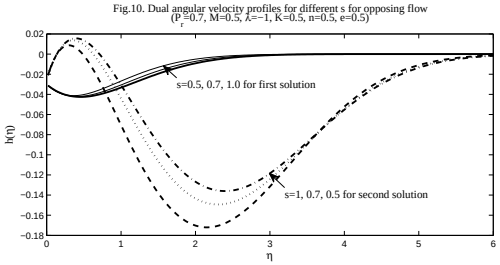

Figure 10

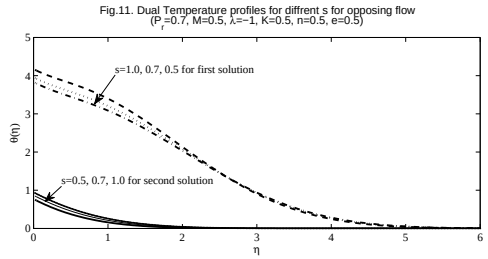

Figure 11

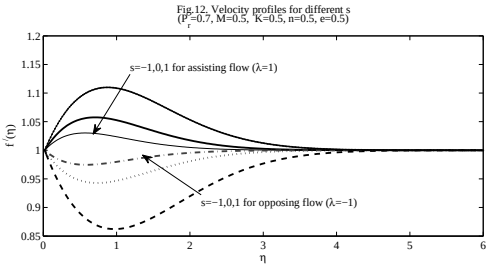

Figure 12

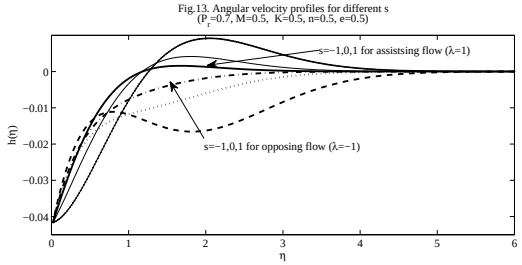

Figure 13

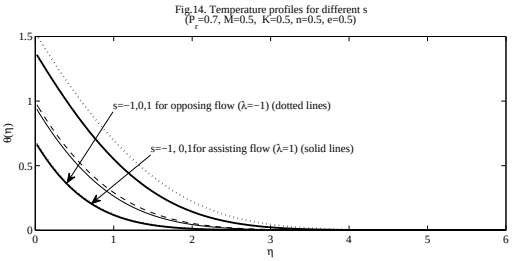

Figure 14

5. Conclusions

A numerical study is performed for the problem of the steady laminar mixed convection boundary layer flow on a vertical surface under prescribed heat flux. The velocity, angular velocity and temperature

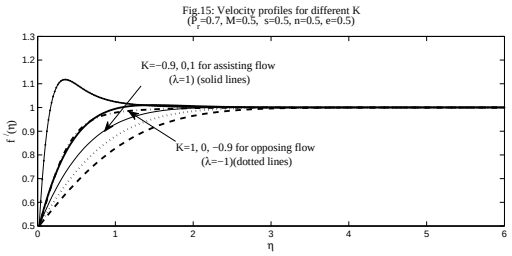

Figure 15

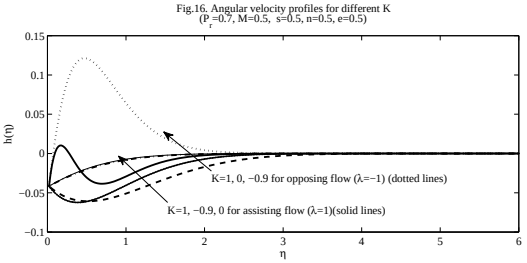

Figure 16

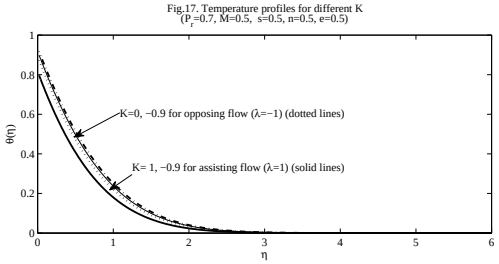

Figure 17

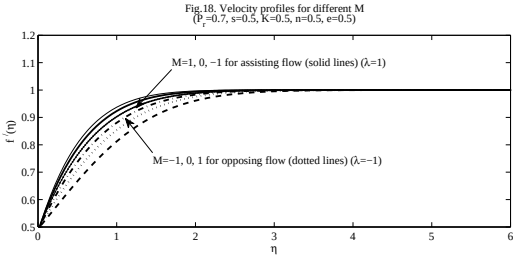

Figure 18

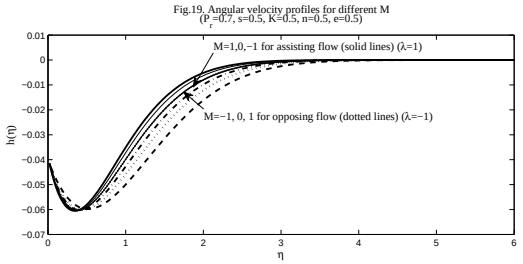

Figure 19

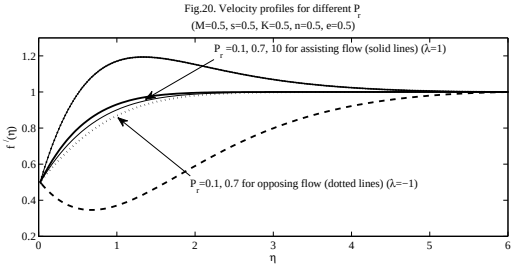

Figure 20

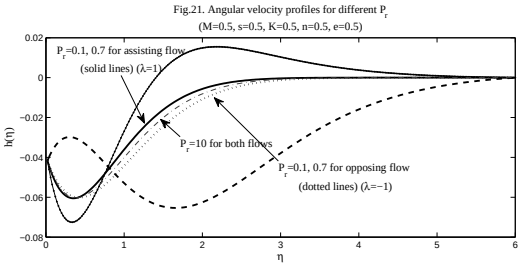

Figure 21

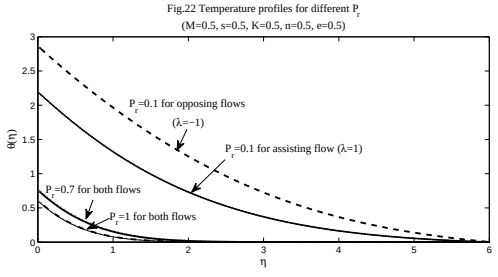

Figure 22

profiles are affected by the suction parameter, magnetic parameter, material parameter, Prandtl number and the buoyancy parameter for both assisting and opposing flows. The following observations are maid:

1. Suction, magnetic field and micropolar fluids delay the boundary-layer separation as compared to

the non-suction, non-magnetic field and the classical Newtonian fluids respectively.

2. Suction, magnetic field and micropolar fluids show drag reduction compared to the non-magnetic field and classical Newtonian fluids respectively.

3. Dual similarity solutions are found to exist for the opposing flow, while for the assisting flow, the solution is unique. The first solutions are stable with the most physically relevance while the second solutions are not.

4. Velocity profiles decrease for the assisting flow but the profile increase for the opposing flow with the increase of suction parameter and Prandtl number. The profiles decrease with the increase of material parameter but increase with the increase of magnetic parameter for the both flows. When Pr=10 the velocity profiles are same for the both flows.

5. For the assisting flow angular velocity profiles increase near boundary but after a certain point the profiles decrease with the increasing of suction parameter and Prandtl number and for the opposing flow the profiles increase with the increasing of suction parameter. The profiles decrease with the increasing of material parameter and for the Newtonian fluid (K=0) the profiles are same for the both flows. When K=1 angular velocity profile for the assisting flow is higher than the opposing flow but the reverse result occurs when K=-0.9. These profiles increase with the increase of magnetic parameter for the both flows. When Pr=10 these profiles are same for the both flows.

6. Temperature profiles decrease with the increasing of suction parameter, of material parameter, Prandtl number for the both flows. When Pr=0.1 temperature profile for the assisting flow is lower compared to the opposing flow but when Pr=0.7 or 1, temperature profiles are same for the both flows

Acknowledgements: The author gratefully acknowledges the financial support received from the UGC, India (Minor Research Project: PSW 145/11-12 (ERO) 25 Jan 12).

References

[1] A.C. Eringen, Theory of Micropolar Fluids, *Jr. Math. Mech.*, **16**, (1966), 1-18.
[2] A.C. Eringen, Theory of Thermomicropolar Fluids, *Jr. Math. Appl.*, **38**, (1972), 480-495.
[3] M.M. Khonsari, On the self-excited whirl orbits of a journal in a sleave bearing lubricated with micropolar fluids, Acta Mech., **81**, (1990), 235-244.
[4] B. Hadimoto and T. Tokioka, Two-dimensional shear flows of linear micropolar fluids, Int. Jr. Engg. Sci., **7**, (1969), 515-522.
[5] J.D. Lee and A.C. Eringen, Boundary effects of orientation of nematic liquid crystals, Jr. Chem. Phys., **55**, (1971), 4509-4512.
[6] T. Ariman , M.A. Turk and N.D. Sylvester, Microcontinuum fluid mechanics- review, *Int. Jr. Engg. Sci.*, **11**, (1973)905-930.
[7] V. Kolpashchikov, N.P. Migun and P.P. Prokhorenko, Experimental determinations of material micropolar coefficients, Int. Jr. Engg. Sci., **21**, (1983), 405-411.
[8] T. Ariman , M.A. Turk and N.D. Sylvester, Application of Microcontinuum fluid mechanics, *Int. Jr. Engg. Sci.*, **12**, (1974) 273-293.
[9] Yücel, Mixed convection in micropolar fluid flow over a horizontal plate with surface mass transfer, *Int. Jr. Engg. Sci.* **27**, (1989), 1593-1602.
[10] S.K. Jena and M.N. Mathur, Similarity solution for laminar free convection flow of thermomicropolar fluid past a non-isothermal vertical flat plate, Int. Jr. Engg. Sci., **19**, (1981), 1431-1439.
[11] R.S.R. Gorla, Combined forced and free convection in micropolar boundary layer flow on a vertical flat plate, Int. Jr. Engg. Sci, **26**, (1983), 385-391.

[12] M.A. Hossain, M.K. Chowdhury and H.S. Takhar, Mixed convection flow of micropolar fluids with variable spin gradient viscosity along a vertical plate, Jr. Theo. Appl. Fluid Mech., **1**, (1995), 64-77.
[13] Y. Mori, Buoyancy effects in forced laminar convection flow over a horizontal flat plate, Jr. Heat transfer, **83**, (1961), 479-482.
[14] G. Lukaszewicz, Micropolar fluids: theory and application, (Birkhuser, Basel), (1999).
[15] A.C. Eringen, Microcontinuum field theories, II. Fluent Media, (Springer, New York), (2001).
[16] A. Ishak , R. Nazar and I. Pop, Magnetohydrodynamic stagnation point flow towards a stretching vertical sheet in a micropolar fluid, *Magnetohydrodynamic* **43**, (2007), 83-97.
[17] A. Ishak, R. Nazar and I. Pop, Mixed convection stagnation point flow of a micropolar fluid towards a stretching sheet , *Mechanica* **43**, (2008), 411-418.
[18] N. Ramachandran, T.S. Chen and B.F. Armaly, Mixed convection in stagnation flows adjacent to a vertical surfaces, *ASME Jr. Heat Transfer*, **110**, (1988), 373-377.
[19] C.D.S. Devi, H.S. Takhar, and G. Nath, Unsteady mixed convection flow in stagnation region adjacent to a vertical surface, *J. Heat Mass Transfer*, **26**, (1991), 71-79.
[20] Y.Y. Lok, N. Amin, D. Campean and I. Pop, Steady mixed convection flow of a micropolar fluid near the stagnation point on a vertical surface, *Int. Jr. Num. Methods Heat Fluid Flow* **15**, (2005), 654-670.
[21] T.R. Mahapatra and A.S. Gupta, Magnetohydrodynamic stagnation point flow towards a stretching sheet, Acta Mech., **152**, (2001), 191-196.
[22] C.H. Chen, Combined effects of Joule heating and viscous dissipation on Magnetohydrodynamic flow past a permeable stretching surface with free convection and radiative heat transfer, ASME Jr. Heat transfer, **132**, (2010), P064503.
[23] K.E. Chin, R. Nazar, N. Arifin and I. Pop, Effect of variable viscosity on mixed convection boundary layer flow over a vertical surface embedded in a porous medium, *Int. Comm. Heat Mass Transf.*, **34**, (2007), 464-473.
[24] S.C. Ling, R. Nazar and I. Pop, Steady mixed convection boundary layer flow over a vertical flat plate in a porous medium filled with water at 4^0C: case of variable wall Temperature, *Trans. Porous Med.*, **69**, (2007), 359-372.
[25] K. Das, Hydromagnetic thermal boundary layer flow of a perfectly conducting fluid, Turk Jr. Phy., 35 (2011), 161-171.
[26] S. Mukhopadhyay, S. Uddin and G.C. Layek, Lie group analysis of MHD boundary layer slip flow past a heated stretching sheet in presence of Heat source/sink, Int. Jr. Appl. Math. & Mech., 8(16), (2012), 51-66.
[27] G.C. Shit and R. Halder, Thermal radiation effects on MHD viscoelastic fluid flow over a stretching sheet with variable viscosity, Int. Jr. of Appl. Math. & Mech., 8(14), (2012), 14-36.
[28] A. Adhikari and D.C. Sanyal, Heat transfer on MHD viscous flow over a stretching sheet with prescribed heat flux, *Bull. Int. Math. Virtual Instt.*, **3**, (2013), 35-47.
[29] K.R. Cramer, Several Magnetohydrodynamic free convection solutions, ASME Jr Heat Transfer, **85**, (1963), 35-40.
[30] M.H. Cobble, Free convection with mass transfer under the influence of a magnetic field, Nonlinear Anal. Theo. Methods Appl., **3**, (1979), 135-143.
[31] A. Raptis, C. Perdikis and G. Tziranidis, Effects of free convection currents on the flow of an electrically conducting fluid past an accelerated vertical infinite plate with variable suction, Jr. Appl. Mech., **61**, (1981), 341-342.
[32] M. Kumari, A. Slaouti, H.S. Takhar, S. Nakamura and G. Nath, Unsteady free convection flow over a continuous moving vertical surface, Acta Mech., **116**, (1996), 75-82.
[33] G. Ahmadi, Self-similar solution of incompressible micropolar boundary layer flow over a semi-infinite flat plate, *Int. Jr. Engg. Sci.*, **14**, (1976), 639-646.
[34] D.A.S. Rees and A.P. Bassom, The Blasius boundary-layer flow of a micropolar fluid, *Int. Jr. Engg. Sci.* **34**, (1996), 113-124.
[35] T. Cebeci and P. Bradshaw, Physical and Computational Aspects Convective Heat Transfer, (Springer, New York), (1988).
[36] N. Bachok and A. Ishak, MHD stagnation-point flow of a Micropolar Fluid with Prescribed Wall Heat Flux, *European Jr. of Sci. Research*, **35**(3), (2009), 436-443.